Bulletin of Pure and Applied Sciences
Section - E - Mathematics & Statistics
Website : https : //www.bpasjournals.com/

Bull. Pure Appl. Sci. Sect. E Math. Stat.
38E(2), 550–562 (2019)
e-ISSN:2320-3226, Print ISSN:0970-6577
DOI: 10.5958/2320-3226.2019.00056.0

Numerical study on the effect of linear/non-linearly stretching sheet with suction or injection of MHD mixed convection Jeffrey fluid flow in a vertical stagnation - point of a porous medium in the presence of thermal radiation and chemical reaction *

G. Kathyayani[1] and R. Lakshmi Devi[2]

1. Department of Applied Mathematics, Yogi Vemana University,
Kadapa, Andhra Pradesh-516216, India.
2. Research Scholar, Department of Applied Mathematics, Yogi Vemana University,
Kadapa, Andhra Pradesh-516216, India.
1. E-mail: kathyagk@gmail.com , 2. E-mail: lakshmi.rathiraju@gmail.com

Abstract The effects of linear /non-linearly stretching sheet with MHD mixed convection Jeffrey fluid flow in a vertical stagnation-point of a porous medium is numerically studied. The influence of thermal radiation, chemical reaction and slip is also considered in this study. The partial momentum and energy equations are transformed into a set of ordinary differential equations by employing suitable similarity transformations and are solved numerically using the Runge-Kutta fourth order method in association with the shooting technique in MATLAB. The effects of Jeffrey parameter, suction/injection parameter, slip velocity parameter, linearity or non-linearity parameter, magnetic parameter, permeability parameter, velocity ratio parameter, Prandtl number, thermal radiation parameter, chemical reaction parameter and Eckert number on velocity, temperature and concentration profiles are presented graphically while the skin friction coefficient, the local Nusselt number and Sherwood number are represented numerically.

Key words Chemical reaction, Jeffrey parameter, MHD mixed convection, non-linearly stretching sheet, Porous medium, slip flow, Thermal radiation, Viscous dissipation.

2010 Mathematics Subject Classification 76W05, 76W99, 76V05, 76V99, 76S05, 76S99.

1 Introduction

Stagnation flow is the name given to the fluid flow near a stagnation-point. In the stagnation area the fluid pressure and the rates of heat and mass transfer are the highest. The stagnation-point flow has much importance due to stretching sheet because its crucial practical applications consist of glass fiber, cooling of metallic plates, extrusion of polymers and aerodynamics. The study of MHD stagnation-point flow in stretching sheet has attracted many researchers in recent periods and many problems are discussed in different areas like pharmaceutical, physiology, fiber technology, crystal growth industry

* Communicated, edited and typeset in Latex by *Lalit Mohan Upadhyaya* (Editor-in-Chief).
Received December 08, 2018 / Revised April 28, 2019 / Accepted May 17, 2019. Online First Published on December 24, 2019 at https://www.bpasjournals.com/.
Corresponding author G. Kathyayani, E-mail: kathyagk@gmail.com

and engineering such as polymer extrusion, cooling of electronic devices and nuclear reactors and drawing of plastic sheets. The slip flow regime is called the flow regime and its effect cannot be neglected. The problem of the slip flow regime is very significant in this area of technology, modern science and tremendous ranging industrialization. The study of convective heat transfer through porous medium for an incompressible fluid on the heated surface has received major attention because of its diverse uses in the insulation of nuclear reactors, geothermal problems, petroleum industry, storage of nuclear waste, and several other areas. Many industrial as well as biological fluids such as blood, paints, fruit juices, polymers, ceramics, multi-grade oils, printer inks, lubricating greases, liquid detergents, etc. change the Newton's law of viscosity. Different models of non-Newtonian fluids based on their diverse flow behaviors are proposed by the researchers.

The study of MHD mixed convection flow near the stagnation-point flow on stretching sheet has attracted many researchers in recent times and many problems are discussed in different aspects (linear or non-linear and suction/injection) including the effect of slip by [1–6]. Ramachandran et al. [7], Wang [8], Abel and Mahesha [9], Labropulu and Li [10] and Hsiao [11] examined the effect of slip flow of a non-Newtonian fluid behavior at a stagnation-point over a stretching sheet with suction or injection. Mahanta and Shaw [12] investigated the MHD Casson fluid flow over a linearly stretching porous sheet with convective boundary. Chaudhary and Kumar [13], Aman et al. [14], Sin Wei Wong et al. [15] and Shen et al. [16] analyzed the steady $2-D$ MHD boundary-layer flow of a viscous, incompressible and electrically conducting fluid near a stagnation-point past a shrinking sheet with slip conditions. Malvandi et al. [17] and Noreen Sher Akbar et al. [18] discussed stagnation point flow of nano fluid towards a stretching sheet in the presence of heat generation/absorption. Unsteady MHD flow near a stagnation point of two-dimensional porous body with heat and mass transfer in the presence of thermal radiation and chemical reaction is numerically investigated Shateyi and Marewo [19]. Ming Shen et al. [20] investigated on MHD mixed convection flow over a non-linear stretching sheet near a stagnation-point region with velocity slip and prescribed surface heat flux. The results reveal that the increasing exponent of the power-law stretching velocity increases the heat transfer rate at the surface. They also found that the effects of velocity slip and magnetic field increase the rate of heat transfer when the free stream velocity exceeds the stretching velocity, i.e. $\varepsilon < 1$, and they suppress the heat transfer rate for $\varepsilon > 1$.

Fauzi et al. [21] analyzed the effects of the slip parameters on the steady stagnation-point flow and heat transfer due to a shrinking sheet in a viscous and incompressible fluid. It is also found that the velocity slip delays the boundary layer separation whereas the temperature slip does not affect the boundary layer separation. Farooq et al. [22] analyzed the MHD stagnation point flow of a viscoelastic nanofluid towards a stretching surface with nonlinear radiative effects and they noticed that skin friction increases for a larger magnetic parameter. Daniel et al. [23] identified the heat and mass transfer problem with slip, heat and mass convective boundary conditions at the wall for an electrically conducting nano fluid flow due to porous stretching/shrinking sheet. Hayat et al. [24] investigated the flow of an electrically conducting nano fluid over an impermeable stretching cylinder and they presented the effects of double stratification and thermal radiation.

Recently some of the researchers studied in this field like, Shateyi and Marewo [25] investigate numerically MHD mixed convection Jeffery fluid model flow over an exponentially stretching sheet with the influence of thermal radiation and chemical reaction. They are observed that the velocity is enhanced whereas temperature and species concentration are decreasing with increasing values of the Deborah number. Ijaz Khan et al. [26] introduced the novel concept of activation energy in chemically reacting stagnation point flow towards a stretching sheet and they considered cross liquid with transverse magnetic field. Agbaje et al. [27] studied MHD stagnation point flow and heat transfer problem from a stretching sheet in the presence of a heat source/sink and suction/injection in porous media and their results are benchmarked with previous results. Other pertinent references concerning the effect of thermal radiation in the fluid flow in porous medium are those of Anwar et al. [29] and Raptis [30] .

Enthused by the above applications and surveys explained, the purpose of this present study is to investigate numerically the effects of linearly or non-linearly stretching sheet on MHD mixed convection stagnation-point of Jeffrey fluid flow with chemical reaction in a vertical plate embedded in a porous medium. The chemical reaction and porous medium are included in the study of Stanford Shateyi and Fazle Mabood [28]. The results are presented through graphs and tabular form. The results for special cases are also compared with those by Stanford Shateyi and Fazle Mabood [28] and Wang [8].

Approximations of skin friction, the Nusselt number and Sherwood number which play a very vital role in engineering applications are also discussed. It is hoped that the results obtained in this study will serve as a complement to the previous studies and also provide useful information for further studies.

2 Mathematical formulation of the problem

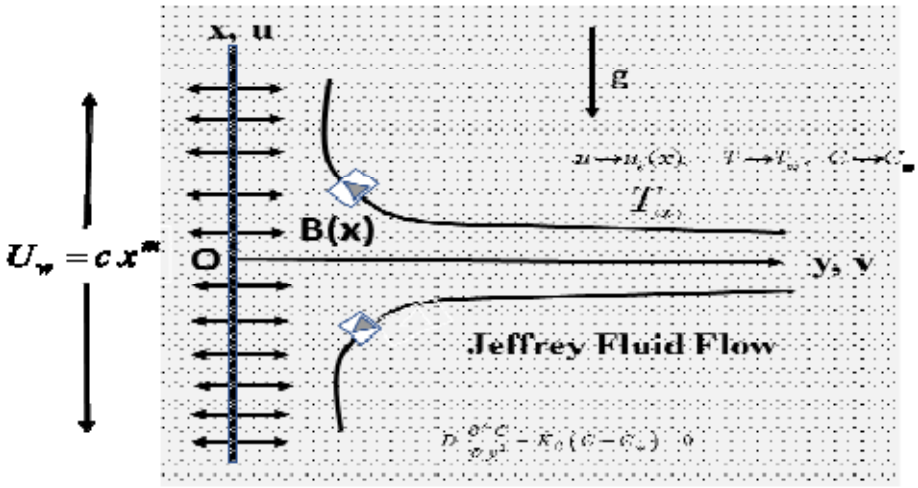

Fig. 1: Physical Model.

We study numerically, the effects of linear or non-linearly stretching sheet of MHD mixed convection stagnation-point of Jeffrey fluid flow in a vertical plate embedded in a porous medium with slip. We consider the influence of thermal radiation and chemical reaction with suction or injection. The axis is taken along the continuous stretching surface in the direction of motion with the slot as the origin and the $y-$axis is perpendicular to it and the flow is confined in the half plane $y > 0$. A uniform magnetic field of strength $B(x)$ is applied in the direction normal to the surface is as shown in Fig. 1. The stretching sheet velocity is assumed to be $u_w(x) = c\,x^m$and the external velocity is prescribed as $u_e(x) = a\,x^m$, where c and a are positive constants. While m is the non-linear parameter, with $m = 1$ for the linear case and $m \neq 1$ for the non-linear case. Under the above assumptions the boundary-layer and Boussinesq approximation are given by [28] as:

$$\frac{\partial u}{\partial x} + \frac{\partial v}{\partial y} = 0 \tag{2.1}$$

$$u\frac{\partial u}{\partial x} + v\frac{\partial u}{\partial y} = u_e\frac{d u_e}{d y} + \frac{\upsilon}{1+\lambda_1}\frac{\partial^2 u}{\partial y^2} - \frac{\sigma B^2(x)}{\rho}(u_e - u) - \frac{\upsilon}{K}u + g\beta\,(T - T_\infty) + g\beta_C\,(C - C_\infty) \tag{2.2}$$

$$u\frac{\partial T}{\partial x} + v\frac{\partial T}{\partial y} = \alpha\,\frac{\partial^2 T}{\partial y^2} - \frac{1}{\rho\ Cp}\frac{\partial q_r}{\partial y} + \frac{\mu}{\rho Cp}\left(\frac{\partial u}{\partial y}\right)^2 \tag{2.3}$$

$$u\frac{\partial C}{\partial x} + v\frac{\partial C}{\partial y} = D\,\frac{\partial^2 C}{\partial y^2} - K_C\,(C - C_\infty) \tag{2.4}$$

where u and v are the velocity components in the $x-$ and $y-$ directions respectively,$\mu-$ the dynamic viscosity, $\upsilon-$ the kinematic viscosity, λ_1- the Jeffrey fluid flow, $\rho-$ the fluid density, $\sigma-$ the electrical conductivity, $B(x)-$ the transverse magnetic field, $K-$ the porous medium parameter, $g-$ the acceleration due to gravity, $\beta-$ the thermal expansion coefficient, β_c- the solutal expansion coefficient, $T-$ the fluid temperature, $\alpha-$ the thermal diffusivity, C_p- the heat capacity at constant pressure, q_r-

the radiative heat flux, $D-$ the mass diffusivity and $K_c$is the chemical reaction rate constant. The associated boundary conditions for the current model are given by:

$$u = u_w(x) + \frac{2-\delta_v}{\delta_v}\lambda_0 \frac{\partial u}{\partial x}, \quad v = v_w(x), \quad \frac{\partial T}{\partial y} = -\frac{q_w(x)}{k}, \quad \frac{\partial C}{\partial y} = -\frac{C_w(x)}{K_C} \quad \text{at } y = 0 \tag{2.5}$$

$$u \to u_e(x), \qquad T \to T_\infty, \quad C \to C_\infty \quad \text{as } y \to \infty \tag{2.6}$$

where δ_v is the tangential momentum accommodation coefficient, λ_0 – the mean free path, $v_w(x)-$ the suction or injection velocity, $k-$ the thermal conductivity, and q_w- the surface heat flux. By using the Rosseland diffusion approximation, and following Hossain et al. [29] and Raptis [30] besides other researchers, the radiative heat flux q_r is given by:

$$q_r = -\frac{4\sigma^* T_\infty^3}{3K_s}\frac{\partial T^4}{\partial y} \tag{2.7}$$

where σ^* and K_s are the Stefan-Boltzman constant and the Rosseland mean absorption coefficient respectively. We assume that the temperature differences within the flow are sufficiently small so that T^4 may be expressed as a linear function of temperature, T.

$$T^4 \approx 4T_\infty^3 T - 3T_\infty^3 \tag{2.8}$$

Using (2.7) and (2.8) in the fourth term of (2.3) we obtain:

$$\frac{\partial q_r}{\partial y} = -\frac{16\sigma^* T_\infty^3}{3K_s}\frac{\partial^2 T}{\partial y^2} \tag{2.9}$$

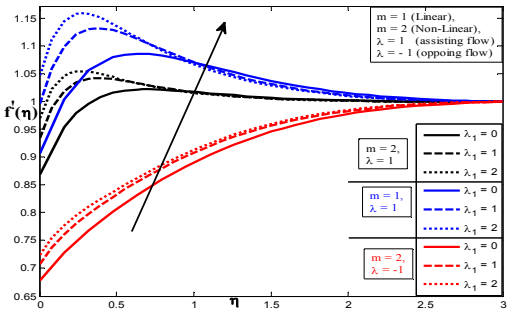

Fig. 2: Velocity profile for different values of Jeffrey fluid parameter λ_1.

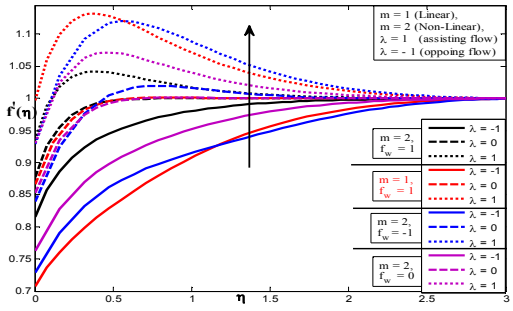

Fig. 3: Velocity profile for different values of mixed convection parameter λ.

3 Similarity analysis

We introduce the following similarity transformations:

$$\eta = \sqrt{\frac{a}{v}} y x^{\frac{m-1}{2}}, \psi = \sqrt{av} x^{\frac{m+1}{2}} f(\eta), \theta = \sqrt{\frac{a}{v}} \frac{k(T-T_\infty)}{q_0 x^{2m-1}}, \phi = \sqrt{\frac{a}{v}} \frac{K_C(C-C_\infty)}{C_0 x^{2m-1}} \tag{3.1}$$

here ψ is the stream function such that $u = \frac{\partial \psi}{\partial y}$, $v = -\frac{\partial \psi}{\partial x}$ and continuity equation is automatically satisfied. By using (3.1), the velocity components u and v are given:

$$u = ax^m f'(\eta), v = -\sqrt{av} x^{\frac{m-1}{2}} \left[\frac{m+1}{2} f(\eta) + \frac{m-1}{2}\eta f'(\eta)\right] \tag{3.2}$$

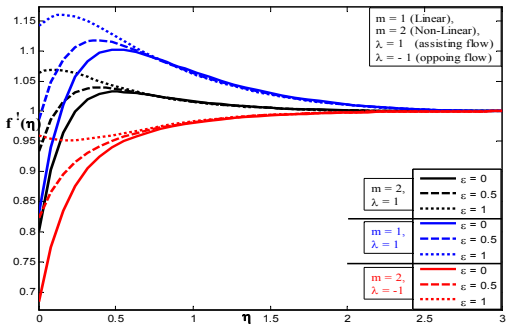

Fig. 4: Velocity profile for different values of velocity ratio parameter ε.

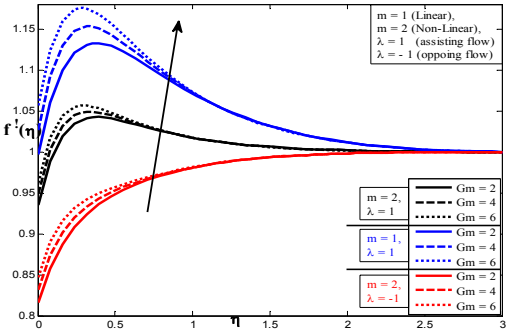

Fig. 5: Velocity profile for different values of Grashof number Gm.

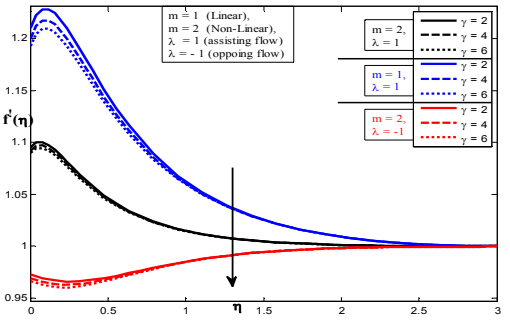

Fig. 6: Velocity profile for different values of the chemical reaction parameter γ.

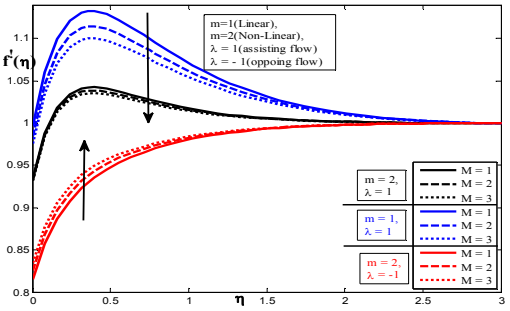

Fig. 7: Velocity profile for different values of magnetic parameter M.

where the primes denote differentiation with respect to η. We remark that to obtain the similarity solutions $B(x)$, $v_w(x)$, $q_w(x)$ and $C_w(x)$ are taken:

$$B(x) = B_0 x^{\frac{m-1}{2}}, v_w = -\frac{\sqrt{av}\,(m+1)}{2} x^{\frac{m-1}{2}} f_w, q_w(x) = q_0 x^{\frac{5m-1}{2}}, C_w(x) = C_0 x^{\frac{5m-1}{2}} \tag{3.3}$$

where B_0, f_w, q_0 and C_0 are arbitrary constants. Also, we have $f_w > 0$ and $f_w < 0$ corresponding to the injection case and implying suction. Upon substituting the similarity variables into (2.2) – (2.4), we obtain the following system of ODE:

$$\frac{1}{(1+\lambda_1)} f''' + \left(\frac{m+1}{2}\right) f f'' - m\left(1 - f'^2\right) - \left(\frac{1}{K} + M\right)\left(1 - f'\right) + \lambda\theta + Gm\phi = 0 \tag{3.4}$$

$$\left(1 + \frac{4}{3R}\right)\theta'' + \Pr\left\{\left(\frac{m+1}{2}\right) f\theta' - (2m-1) f'\theta + Ec\left(f''\right)^2\right\} = 0 \tag{3.5}$$

$$\phi'' + Sc\left\{\left(\frac{m+1}{2}\right) f\phi' - (2m-1) f'\phi - \gamma\phi\right\} = 0 \tag{3.6}$$

The corresponding boundary conditions for the transformed equations are:

$$f(0) = f_w, f'(0) = \varepsilon + \delta f''(0), \theta'(0) = -1, \phi'(0) = -1 \tag{3.7}$$

$$f'(\infty) = 1, \theta(\infty) = 0, \phi(\infty) = 0 \tag{3.8}$$

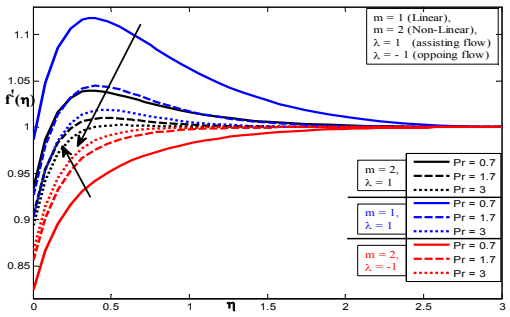

Fig. 8: Velocity profile for different values of Prandtl number Pr.

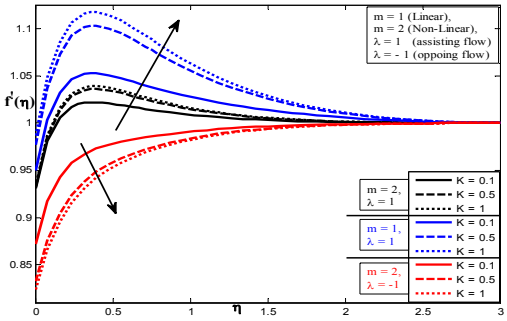

Fig. 9: Velocity profile for different values of porous medium parameter K.

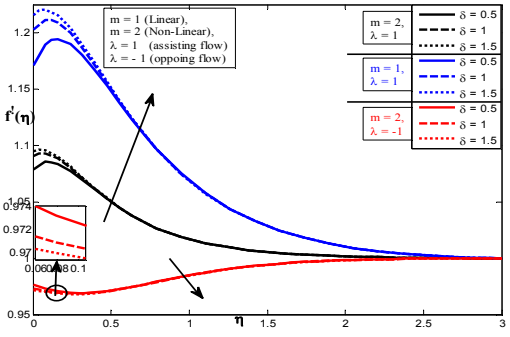

Fig. 10: Velocity profile for different values of slip parameter δ.

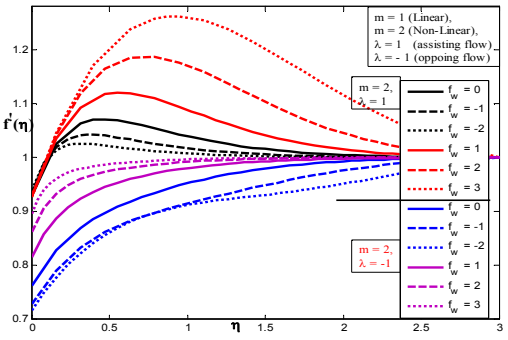

Fig. 11: Velocity profile for different values of Injection/suction parameter f_w.

We have $M = B_0^2/\rho a$ the magnetic parameter, $\lambda = \frac{g\beta q_0\sqrt{v}}{ka}$ the mixed convection parameter, $\Pr = v/\alpha$ the Prandtl number, $R = 4\sigma^* T^3/\rho C_p k_1$ is the thermal radiation parameter,$Sc = \frac{v}{D}$ is the Schmidt number, $\gamma = \frac{Kcv}{x^{2m-1}}$ is the chemical reaction parameter, $K = \frac{k\,a\,x^{m-1}}{v}$ is the porous medium parameter, $Gm = \frac{v\,g\,\beta_c(C-C_\infty)}{x^{2\,m-1}}$ is the mass Grashof number, $Ec = a^{5/2}x^{3m}\big/\rho C_p$ is the Eckert number, $\varepsilon = c/a$ is the velocity ratio parameter, $\delta = (2-\sigma_v)\,kx_n Re_x^{1/2}\big/\sigma_v$ is the velocity slip parameter.

4 Local skin friction, Nusselt number and Sherwood number

The parameters of physical interest for the present problem are the local skin friction coefficient C_f, the local Nusselt number Nu_x and local Sherwood number Sh_x which are defined as:

$$C_f = \frac{\tau_w(x)}{\rho\,(1+\lambda_1)\,u_p^2}, Nu_x = \frac{xq_w(x)}{k(T_w - T_\infty)}, Sh_x = \frac{xc_w(x)}{K_C(C - C_\infty)} \tag{4.1}$$

with the surface shear stress $\tau_w(x) = \partial u/\partial y]_{y=0}$,$q_w(x)$ and $C_w(x)$ is the wall heat flux. We then obtain the following expressions after applying the similarity variables:

$$Re_x^{1/2} C_f = \frac{f''(0)}{(1+\lambda_1)}, Re_x^{1/2} Nu_x = \theta'(0), Re_x^{1/2} Sh_x = \phi'(0) \tag{4.2}$$

where $Re_x = u_e x/v$ be the Reynolds number and the numerical values of the functions $f''(0), \theta'(0)$, and $\phi'(0)$ represent the wall shear stress, the heat transfer rate and the local Sherwood number at the

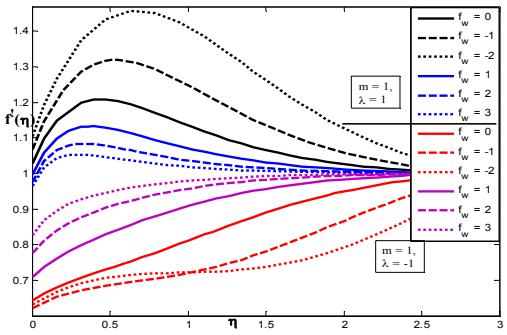

Fig. 12: Velocity profile for different values of Injection/suction parameter f_w.

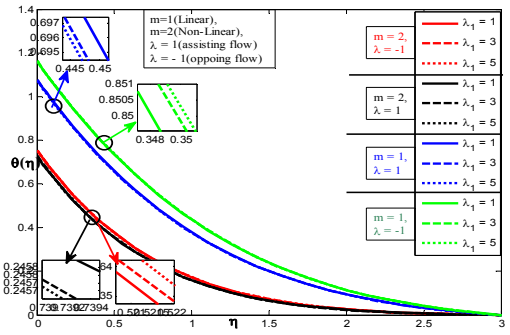

Fig. 13: Temperature profile for different values of Jeffrey fluid parameter λ_1.

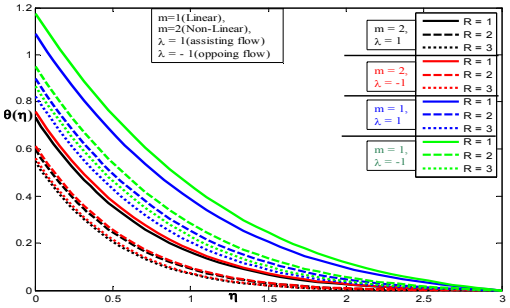

Fig. 14: Temperature profile for different values of thermal radiation parameter R.

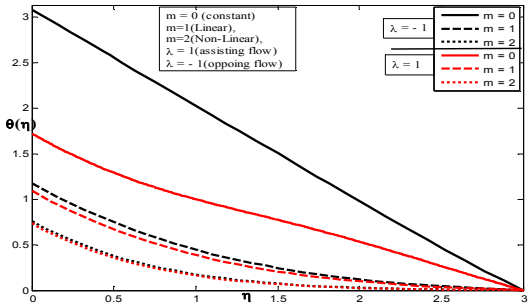

Fig. 15: Temperature profile for different values of the non-linear parameter m.

surface respectively for the various values of the parameters which are presented in Table 1.

5 Results and discussion

In this paper, the effects of linear or non-linear stretching and suction or injection of MHD mixed convection Jeffrey fluid flow in a vertical stagnation-point embedded in a porous medium are analyzed. The influence of thermal radiation, chemical reaction and slip is also considered in this study. The momentum and governing equations are solved numerically by shooting technique with Runge-Kutta fourth order using MATLAB. The effects of the linear or non-linear parameter m vary with m ($m = 1$ or $m = 2$), the suction/injection parameter f_w, the Magnetic parameter M, the Jeffrey parameter λ_1, the velocity slip parameter δ, the porous medium parameter K, the velocity ratio parameter ε, the Prandtl number Pr, the Eckert number Ec, the thermal Radiation parameter R, the mixed convection parameter λ, the mass Grashof number Gm and the chemical reaction parameter γ, the Schmidt number Sc are depicted through graphs on velocity $f'(\eta)$, temperature $\theta(\eta)$ and concentration $\phi(\eta)$ profiles with fixed values of m ($m = 1$ or $m = 2$),$f_w = 1$, $M = 2$,$\lambda_1 = 1$, $\delta = 1$, $K = 1$, $\varepsilon = 0.5$, Pr $= 0.7$, $Ec = 1$, $R = 1$, $\gamma = 1$,$\lambda = 1$ and $\gamma = 1$. In order to compute the values of Skin friction coefficient $\frac{f''(0)}{1+\lambda_1}$, local Nusselt number$-\theta'(0)$ and Sherhood number $\phi'(0)$ are compared with the available results of Stanford Shateyi and Fazle Mabood [28] and Wang [8] in Table 1 and have found in excellent agreement. The numerical results with graphical representations are illustrated in Figs. 2 – 24. From the Figs. 2, 3, 4 and 5 it is seen that the effects of Jeffrey parameter λ_1, mixed convection parameterλ, velocity ratio

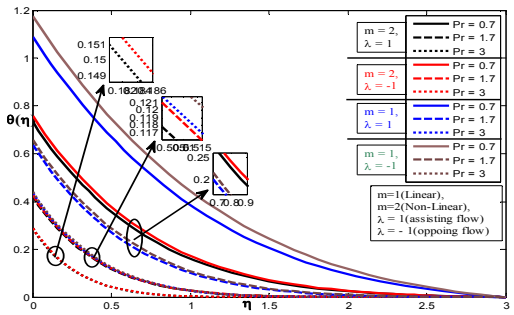

Fig. 16: Temperature profile for different values of thermal radiation parameter R.

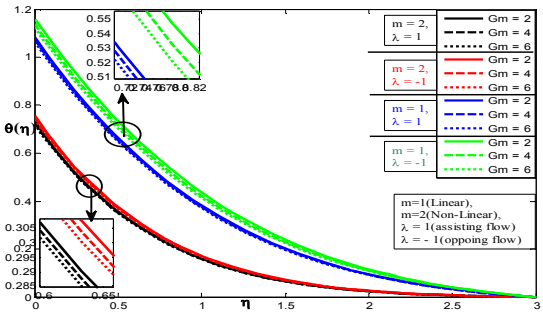

Fig. 17: Temperature profile for different values of the non-linear parameter m.

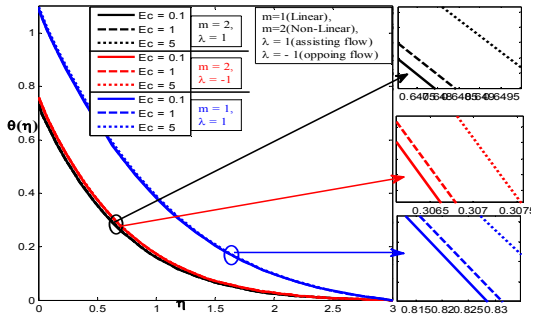

Fig. 18: Temperature profile for different values of Eckert number Ec.

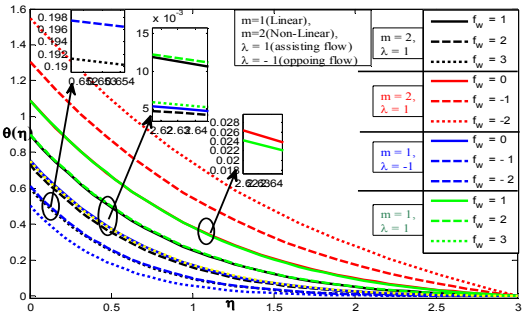

Fig. 19: Temperature profile for different values of injection/suction parameter f_w.

parameter ε and mass Grashof number Gm on the velocity profiles for both assisting and opposing cases vary with linear ($m = 1$) and non-linear ($m = 2$). It is observed that the velocity increases with an increase in the Jeffrey parameter λ_1, the mixed convection parameter λ, the velocity ratio parameter ε and the mass Grashof number Gm for all the cases of linearity ($m = 1$), non-linearity($m = 2$) vary with assisting flow ($\lambda = 1$) and opposing flow ($\lambda = -1$). Also it is observed that the velocity attains the maximum value at $m = 1$ and $\lambda = 1$. The opposite behavior is observed for the chemical reaction parameter γ from the Fig. 6.

Figures 7 and 8 represent the effects of the Magnetic parameter M and the Prandtl number Pr on the velocity profiles for both the assisting ($\lambda = 1$) and opposing ($\lambda = -1$) cases vary with linear ($m = 1$) and non-linear ($m = 2$). It can be seen that with an increase of M and Pr the velocity decreases for the case of assisting flow $\lambda = 1$ vary with $m = 1$ and $m = 2$. The opposite behavior is observed in the case of opposing flow $\lambda = -1$ varying with $m = 2$. The Figs. 9 and 10 represent the influence of porous medium parameter K and the velocity slip parameter δ, on the velocity profiles for both assisting ($\lambda = 1$) and opposing ($\lambda = -1$) cases vary with linear ($m = 1$) and non-linear ($m = 2$). It can be seen that with the increase of K and δ, the velocity increases for the case of assisting flow $\lambda = 1$ varying with $m = 1$ and $m = 2$ while the opposite behavior is observed in the case of opposing flow $\lambda = -1$ varying with $m = 2$. Figs. 11 and 12 depict the encouragement of suction/injection parameter f_w, on the velocity profiles for both assisting and opposing cases vary with the linear ($m = 1$) and non-linear ($m = 2$) cases. It can be seen from the Fig. 11 that the velocity increases with increasing values of f_w ($= 1, 2, 3$), for the case of $\lambda = 1$, $\lambda = -1$varying with $m = 2$ and also the opposite behavior

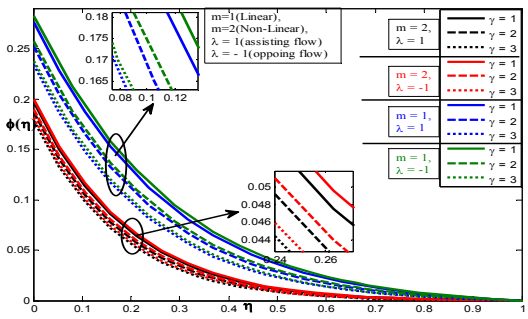

Fig. 20: Concentration profile for different values of the chemical reaction parameter γ.

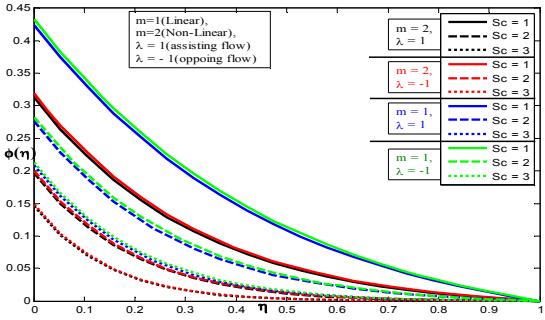

Fig. 21: Concentration profile for different values of the Schmidt number Sc.

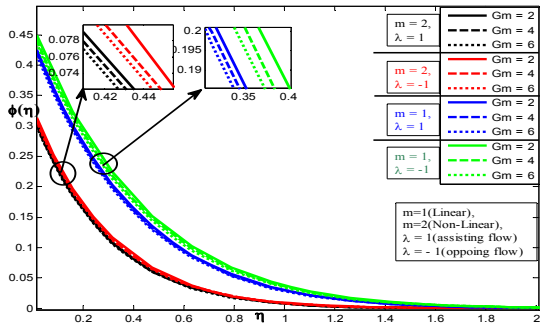

Fig. 22: Concentration profile for different values of the Grashof number Gm.

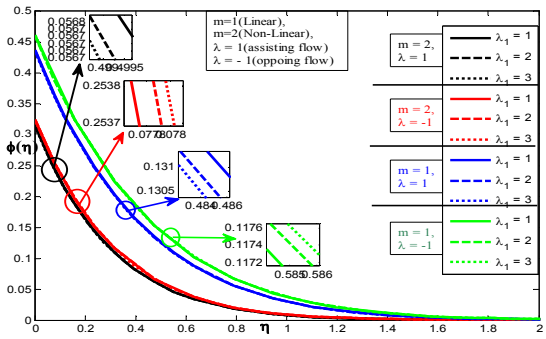

Fig. 23: Concentration profile for different values of the Jeffrey fluid parameter λ_1.

is observed for the values of $f_w\,(=0,-1,-2)$. From the Fig. 12, the velocity increases with a decrease in f_w in the assisting flow $\lambda = 1$ and the opposite behavior is observed for the opposing flow$\lambda = -1$ varying with $m = 1$.

Fig. 13 depicts the impact of Jeffrey fluid parameter λ_1 on the temperature profile for both the assisting $\lambda = 1$ and the opposing $\lambda = -1$ flow cases varying with linear $m = 1$ and non-linear $m = 2$ cases. It can be seen that the temperature increases with decreasing values of λ_1 for the assisting $\lambda = 1$ flow, and the opposite behavior is observed that for opposing $\lambda = -1$ flow. Figs. 14, 15, 16 and 17 represent the effects of thermal Radiation parameter R, linear or non-linear parameter m, Prandtl number Pr and Grashof number Gm on the temperature profiles for both assisting $\lambda = 1$ and opposing $\lambda = -1$ cases varying with the linear $(m = 1)$ and non-linear $(m = 2)$ cases. It can be seen that decreasing of R, m, Pr and Gm causes the temperature profiles to increase for the case of assisting $\lambda = 1$, and opposing $\lambda = -1$ flow varying with linear $m = 1$ and non-linear $m = 2$. The opposite behavior is observed for the value of Eckert number Ec as shown in Fig. 18. Fig. 19 shows the effects of suction $f_w > 0$, injection parameter $f_w < 0$ on the temperature profiles for both assisting $\lambda = 1$ and opposing $\lambda = -1$ cases varying with the linear $(m = 1)$ and non-linear $(m = 2)$ cases. The temperature decreases with an increasing of $f_w > 0$ and$f_w < 0$ with linear $m = 1$ and non-linearity value $m = 2$. Here the temperature profile attains the maximum value for the values of $m = 2$ and $\lambda = 1$.

Figs. 20, 21 and 22 represent the effects of the chemical reaction parameter γ, the Schmidt number Sc and the mass Grashof number Gm on the concentration profiles for both the assisting $\lambda = 1$ and the

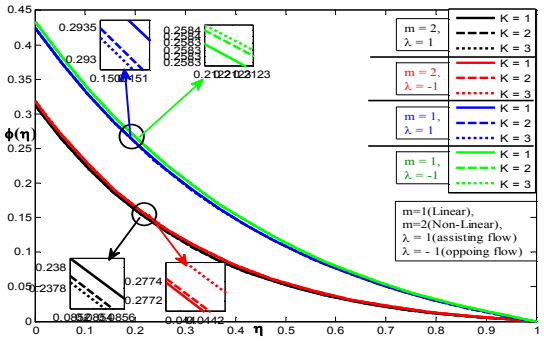

Fig. 24: Concentration profile for different values of the porous medium parameter K.

opposing $\lambda = -1$ cases varying with linear ($m = 1$) and non-linear ($m = 2$) cases. It can be seen that the decreasing of γ, Sc and Gm causes the temperature profiles to increase for the case of assisting $\lambda = 1$, and opposing $\lambda = -1$ flow varying with the linear $m = 1$ and the non-linear $m = 2$ cases. Figs. 23 and 24 represent the effects of the Jeffry fluid parameter λ_1 and the porous medium parameter K on the concentration profiles for both the assisting ($\lambda = 1$) and the opposing ($\lambda = -1$) cases varying with linear $m = 1$ and non-linear $m = 2$ cases. It can be perceived that with the decrease of λ_1 and K, the concentration increases for the case of the assisting flow $\lambda = 1$ varying with $m = 1$ and $m = 2$, the opposite behavior is observed in the case of opposing flow $\lambda = -1$ varying with $m = 1$ and $m = 2$.

6 Conclusions

A numerical model is developed to investigate the effects of linear or non-linearly stretching of MHD mixed convection Jeffrey fluid flow near a stagnation-point towards a vertical plate embedded in a porous medium. The presence of thermal radiation, chemical reaction and slip effects is discussed. The coupled equations boundary value problem is solved here numerically by the shooting technique with Runge-Kutta fourth order using MATLAB. Further numerical results for the skin friction coefficient, the rate of heat transfer at the surface and the Sherwood number are found to be in close agreement with the results which were obtained by earlier researchers in the absence of the Jeffrey parameterλ_1, the porous medium parameter $K$and the chemical reaction parameterγ.

- The governing equations are solved numerically by shooting technique with the Runge-Kutta fourth order method using MATLAB.
- We conclude that the velocity decreases with increase of M, K, Pr, $f_w > 0$ and $f_w < 0$ as well as the temperature decreases with increasing values of R, m, δ, Pr, $f_w > 0$ and $f_w < 0$ and also that the velocity increases with increase of M, λ_1, δ, ε and Ec as well as the temperature increases with increasing of Ec for different aspects ($\lambda = 1$,$\lambda = -1$with $m = 1,\ 2$).
- Table 1 shows that the skin friction coefficient $f''(0)$ increases with the increasing values of the Jeffrey fluid parameter λ_1, the chemical reaction parameter γ and the porous medium parameter K. Further the variation in the values of the rate of heat transfer $\theta'(0)$ at the surface is also shown. From this table it is observed that the rate of heat transfer $\theta'(0)$ decreases with increasing values of the Jeffrey fluid parameter λ_1, the chemical reaction parameter γ and the porous medium parameter K.
- After substituting the parameter values as $\lambda_1 = 0$, $\gamma = 0, K = 0, \delta = \varepsilon = \lambda = M = \Pr = f_w = 1$ in the present results for skin friction and Nusselt number will coincide with the results of Shateyi and Mabood [28]. In addition to this, after substituting the parameter values $\delta = \varepsilon = \lambda = M = \Pr = f_w = \gamma = 0, m = 1$ in the present work we obtain good agreement with

Table 1: Comparison of $-f''(0)$ and $-1/\theta'(0)$ for various values of λ_1 and K and for fixed values of $\lambda_1 = 1$, $M = 2$, $K = 1$, $\delta = 1$, $\varepsilon = 0.5$, Pr $= 0.7$, $Ec = 1$, $f_w = 1$, $(m = 1 \text{ or } m = 2)$ and $\lambda = 1$.

λ_1	γ	K	**Present study** $M = 2,\ \varepsilon = 0.5,\ \Pr = 0.7,\ f_w = Ec = \delta = 1$			**Shateyi and Fazle** [28] $\delta = \varepsilon = \lambda = M = Pr = f_w = 1, \lambda_1 = 0 K = 0,$ γ=0		**Wang** [8] $\delta = \varepsilon = \lambda = M = Pr = \gamma = f_w = 0, \lambda_1 = 0, m = 1$	
			$f''(0)$	$\theta'(0)$	$\phi'(0)$	$f''(0)$	$\theta'(0)$	ε	$f''(0)$
1	2	1	0.2517	1.8926	1.0245	0.1547	1.1196	**0**	1.2342
2	2	1	0.4875	1.8872	1.1257	0.2123	1.0690	**0.1**	1.1454
3	2	1	0.6875	1.7552	1.2672	0.2358	0.9685	**0.2**	1.0122
1	2	**1**	0.6579	1.8952	1.2245	0.1152	1.1176	**0.3**	0.9873
1	2	**2**	0.7187	1.7586	1.2684	0.1587	0.8712	**0.4**	0.8326
1	2	**3**	0.8723	1.6324	1.3625	0.1926	0.7215	**0.5**	0.7252
1	**2**	1	0.7586	1.8926	1.1259	0.1547	1.1196	**0.5**	0.6524
1	**4**	1	0.6875	1.8926	1.3234	0.1547	1.1196	**0.5**	0.6524
1	**6**	1	0.6125	1.8926	1.5246	0.1547	1.1196	**0.5**	0.6524

the existing results of Wang [8].

References

[1] Cheng, J., Liao, S. and Pop, I. (2005). Analytic series solution for steady mixed convection boundary layer flow near the stagnation point on a vertical surface in a porous medium, *Transport in Porous Media*, 61(3), 365–379.

[2] Hayat. T, Abbas. Z., Pop, I. and Asghar, S. (2010). Effects of radiation and magnetic field on the mixed convection stagnation-point flow over a vertical stretching sheet in a porous medium, *International Journal of Heat and Mass Transfer*, 53(1–3), 466–474.

[3] Hayat. T., Qasim. M. and Mesloub, S. (2011). MHD flow and heat transfer over permeable stretching sheet with slip conditions, *Int. J. Numer. Meth. Fluids*, 66(8), 963–975.

[4] Ali, F.M., Nazar, R., Arifin, N.M. and Pop, I. (2014). Mixed convection stagnation-point flow on vertical stretching sheet with external magnetic field, *Appl. Math. Mech.*, 35(2), 155–166.

[5] Takhar. H.S., Chamkha, A.J. and Nath, G. (2005). Unsteady mixed convection on the stagnation-point flow adjacent to a vertical plate with a magnetic field, *Heat and Mass Transfer*, 41(5), 387–398.

[6] Aydin, O. and Kaya. A. (2009). MHD mixed convection of a viscous dissipating fluid about a permeable vertical flat plate, *Applied Mathematical Modelling*, 33(11), 4086–4096.

[7] Ramachandran, N., Chen, T.S. and Armaly, B.F. (1988). Mixed convection in stagnation flows adjacent to vertical surfaces, *ASME Journal of Heat Transfer*, 110(2), 373–377.

[8] Wang, C.Y. (2003). Stagnation flows with slip: exact solutions of the Navier-Stokes equations, *ZAMP*, 54(1), 184–189.

[9] Abel, M.S. and Mahesha, N. (2008). Heat transfer in MHD viscoelastic fluid flow over a stretching sheet with variable thermal conductivity, non-uniform heat source and radiation, *Applied Mathematical Modelling*, 32(10), 1965–1983.

[10] Labropulu, F. and Li, D. (2008). Stagnation-point flow of a second-grade fluid with slip, *International Journal of Non-Linear Mechanics*, 43(9), 941–947.

[11] Hsiao, K.L. (2011). MHD mixed convection for viscoelastic fluid past a porous wedge, *Int. J. Non-Linear Mech.*, 46(1), 1–8.

[12] Mahanta, G. and Shaw, S. (2015). 3D Casson fluid flow past a porous linearly stretching sheet with convective boundary condition, *Alexandria Eng J.*, 54, 653–659.

[13] Chaudhary, S. and Kumar, P. (2013). MHD slip flow past a shrinking sheet, *Appl. Math.*, 4(3), 574–581.

[14] Aman, F., Ishak, A. and Pop, I. (2013). Magnetohydrodynamic stagnation-point flow towards a stretch-ing/ shrinking sheet with slip effects, *Int. Commun. Heat. Mass Transf.* , 47, 68–72.

[15] Wong, Sin Wei, Awang, M.A. Omar and Ishak, Anuar (2013). Stagnation-point flow toward a vertical, nonlinearly stretching sheet with prescribed surface heat flux, *Hindawi Publishing Corporation Journal of Applied Mathematics*, http://dx.doi.org/10.1155/2013/528717.

[16] Shen, Ming, Wang, Fei and Chen, Hui (2015). MHD mixed convection slip flow near a stagnation point on a non-linearly vertical stretching sheet, *Boundary Value Prob.*, 78–92. doi 10.1186/s 13661-015-0340-6.

[17] Malvandi, A., Hedayati, F. and Domairry, G. (2013). Stagnation point flow of a nanofluid toward an exponentially stretching sheet with nonuniform heat generation/absorption, *Hindawi Publishing Corporation Journal of Thermodynamics*, http://dx.doi.org/10.1155/2013/764827

[18] Akbar, Noreen Sher, Nadeem, S. Haq, Rizwan Ul and Khan, Z.H. (2013). Radiation effects on MHD stagnation point flow of nano fluid towards a stretching surface with convective boundary condition, *Chinese Journal of Aeronautics*, 26(6), 1389–1397. http://dx.doi.org/10.1016/j.cja.2013.10.008

[19] Shateyi, Stanford and Marewo, Gerald Tendayi (2014). Numerical analysis of unsteady MHD flow near a stagnation point of a two-dimensional porous body with heat and mass transfer, thermal radiation, and chemical reaction, *Boundary Value Problems*,2, 1–18. http://dx.doi.org/10.1186/s13661-014-0218-z

[20] Shen, Ming, Wang, Fei and Chen, Hui (2015). MHD mixed convection slip flow near a stagnation-point on a non-linearly vertical stretching sheet, *Boundary Value Problems*, 78, 1–15. http://dx.doi.org/10.1186/s13661-015-0340-6

[21] Fauzi, N.F., Ahmad, S. and Pop, I. (2015). Stagnation point flow and heat transfer over a nonlinear shrinking sheet with slip effects, *Alexandria Engineering Journal*, 54, 929–934. http://dx.doi.org/10.1016/j.aej.2015.08.004

[22] Farooq, M., Ijaz Khan, M., Waqas, M., Hayat T., Alsaedi, A. and Khan, Imran M. (2016). MHD stagnation point flow of viscoelastic nanofluid with non-linear radiation effects, *Journal of Molecular Liquids*, 221, 1097–1103. http://dx.doi.org/10.1016/j.molliq.2016.06.077

[23] Daniel, Yahaya Shagaiya, Aziz, Zainal Abdul, Ismail, Zuhaila and Salah, Faisal (2017). Effects of slip and convective conditions on MHD flow of nanofluid over a porous nonlinear stretching/shrinking sheet, *Australian Journal of Mechanical Engineering*, Volume:16,2018; Issue 3; 213–229. http://dx.doi.org/10.1080/14484846.2017.1358844

[24] Hayat, Tasawar, Nassem, Anum, Khan, Muhammad Ijaz, Farooq, Muhammad and Al-Saedi, Ahmed (2017). MHD flow of nanofluid with double stratification and slip conditions, *Physics and Chemistry of Liquids*, http://dx.doi.org/10.1080/00319104.2017.1317778

[25] Shateyi, Stanford and Marewo, Gerald T. (2018). Numerical solution of mixed convection flow of an MHD Jeffery fluid over an exponentially stretching sheet in the presence of thermal radiation and chemical reaction., *Open Phys.*, 16, 249–259. https://doi.org/10.1515/phys-2018-0036

[26] Ijaz Khan, M., Waqas. M., Hayat. T. and Al-saedi, A. (2017). Magneto-hydrodynamical numerical simulation of heat transfer in MHD stagnation point flow of cross fluid model towards a stretched surface, *Physics and Chemistry of Liquids*, http://dx.doi.org/10.1080/00319104.2017.1367791

[27] Agbaje, T.M., Mondal, S., Makukula, Z.G., Motsa, S.S. and Sibanda, P. (2018). A new numerical approach to MHD stagnation point flow and heat transfer towards a stretching sheet, *Ain Shams Engineering Journal*, 9, 233–243. http://dx.doi.org/10.1016/j.asej.2015.10.015

[28] Shateyi, Stanford and Mabood, Fazle (2017). MHD mixed convection slip flow near a stagnation-point on a non-linearly vertical stretching sheet in the presence of viscous dissipation, *Thermal Science*, 21(6B), 2709–2723.

[29] Anwar Hossain, M., Khalil, Khanafer and Kambiz, Vafai (2001). The effect of radiation on free convection flow of fluid with variable viscosity from a vertical porous plate, *Int. J. Therm. Sci.,* 40(2), 115–124.

[30] Raptis, A. (1998). Flow of a micropolar fluid past a continuously moving plate by the presence of radiation, *Int. J. Heat Mass Transf.*, 41(18), 2865–2866.